AN ADAPTIVE RECEIVER FOR STBC IN FREQUENCY SELECTIVE CHANNEL WITH IMPROVED ROBUSTNESS AND PILOT REQUIREMENTS

J. Mathew, H. Xu and F. Takawira

School of Electrical, Electronic and Computer Engineering, University of Kwa-Zulu Natal, King George V Avenue, Durban 4041, South Africa E-mail: xuh, ftakaw@ukzn.ac.za

Abstract: The semi-blind recursive least squares (RLS) based adaptive receiver has been designed to perform joint interference suppression and equalization for space time block codes (STBC) in a frequency and time selective channel. In order to decrease pilot requirements in the training block, this paper introduces a linear predictor (LP) algorithm to do a forward prediction of the channel coefficients based on a smaller pilot block. We then introduce a QR-decomposition (QRD) based algorithm to improve the performance of the receiver at higher Doppler frequencies. The simulation results show that the addition of the LP does not affect the frame error rate (FER) of the overall system. Linear prediction requires a smaller number of pilot symbols in order to provide the channel estimates for a given burst. Hence the LP increases the overall throughput of the system by decreasing the pilot symbols required. The simulation results show that this is a more effective method for improving the system performance as the overall FER of the combined QRD-LP receiver is decreased significantly. Finally, by comparing the QRD based receiver and the RLS based receiver at higher Doppler frequencies, we verify that the QRD receiver has superior FER performance under these conditions.

Keywords: Space time block code, frequency selective channel, adaptive receiver, LP, QR decomposition.

1. INTRODUCTION

Multiple-input multiple-output (MIMO) systems have been proven to significantly increase the capacity in rich scattering environments. The space time block code (STBC), which was first introduced in [1] and later generalized in [2], is an attractive MIMO technique due to its simple linear processing at receiver and because it requires no additional bandwidth. The Alamouti scheme is a special case full rate STBC with two transmit antennas and one receive antenna. The time reversal (TR) STBC [3], orthogonal frequency division multiplexed (OFDM) STBC [4] and single carrier frequency domain equalized (SC-FDE) STBC [5-7] have been proposed in the literature for frequency-selective channels. An overview and comparison of these schemes can be found in [8]. Since OFDM-STBC requires additional outer-coding and interleaving to fully exploit multipath diversity, which results in additional rate loss [9], OFDM-STBC scheme will not be considered in this paper. The other two schemes, which are extensions of the Alamouti's STBC scheme, are getting particular attention because of their ability to exploit the orthogonal structure of STBC over frequency selective channels, keeping the receiver complexity at a manageable level. In [10], TR-STBC was applied to the WCDMA downlink, incorporating chip equalization to suppress multiple access interference (MAI). In [11], TR-STBC was applied to the broadband fixed wireless access systems. More recently, TR-STBC was extended to quasi-orthogonal time-reversal space-time block coding [12]. In the SC-FDE STBC scheme, frequency domain linear equalization has been incorporated into TR-STBC [6-8]. This motivates the use of SC-FDE STBC as a more attractive option.

This paper mainly focuses on the SC-FDE STBC scheme. In the SC-FDE scheme, receivers require channel state information (CSI) at the receiver. One approach is to use training sequences embedded in each block to estimate the CSI. This, however, results in increased system overhead. In addition to this, the mobility of the users may cause the channel impulse response to vary rapidly and hence the quasi-static assumption of the channel becomes void. The use of longer blocks, which is required to reduce the system overhead in such training based schemes, can not be practical in such cases. W. M. Younis in [15-16] developed an efficient low complexity adaptive receiver with fast tracking abilities.

Although the original scheme proposed in [16] is bandwidth efficient in that it does not require the inclusion of pilot symbols in every block, the two key problems identified are as follows:

- There is still the requirement of an entire block of training data to initialize the recursive least squares (RLS) algorithm. An entire block of training data decreases the bandwidth efficiency. Actually, there is a trade off between the performance gain required and the bandwidth efficiency in the scheme proposed in [16].
- The RLS algorithm is not robust, particularly at high Doppler frequencies where there is a significant performance penalty. This is evident from the simulation results in section IV of [15].

The first problem motivates us to develop an algorithm or method to decrease the number of pilot symbols and thus improve the bandwidth efficiency during the re-training interval. The second problem motivates the search for a more robust algorithm at high Doppler frequencies.

The rest of this paper is organized as follows: we begin with the description of the adaptive RLS based receiver [15-16] in section 2. We then describe the linear prediction (LP) algorithm in Section 3. Section 4 details the QRD based adaptive receiver that is used to provide better performance to the RLS algorithm at high Doppler frequencies. We provide simulation results in section 5 and conclude in section 6.

Notations: The following notations are used for the rest of this paper. Upper case letters denote matrices, lower case letters stand for column vectors; $(\cdot)^*$, $(\cdot)^T$ and $(\cdot)^{\mathrm{H}}$ represent conjugate, transpose and Hermitian, respectively; $E[\cdot]$ stands for expectation and $\mathbf{I}_N$ denotes an identity matrix of size $N \times N$. $\mathbf{F}_N$ is for an $N \times N$ discrete Fourier transform (DFT) matrix. $\|\cdot\|$ denotes the Euclidean norm. $\mathrm{Re}\{\cdot\}$ stands for the real part of the term.

2. RLS BASED ADAPTIVE RECEIVER

2.1 Single User Transmission

In the description to follow, it is assumed that each user is equipped with two transmit antennas and one receive antenna. Let the N-symbol block including cyclic prefix (CP) transmitted from the first and second antennas at block time $2i$ be given by x_1 and x_2, respectively. At block time $2i+1$, permuted conjugate versions $-\mathbf{P}x_2^*$ and $\mathbf{P}x_1^*$ are sent from the first and second antennas, respectively. Assuming the original data sequence length and channel length is R and L, respectively, the permutation matrix $\mathbf{P}$ is a circular reversal matrix given by

$$\mathbf{P}=\begin{pmatrix}\mathbf{P}_R\\ \mathbf{P}_L\end{pmatrix}=\begin{pmatrix}1 & 0 & \cdots & 0\\ & \ddots & & \\ 0 & 0 & \cdots & 1\\ \hline 0 & \cdots & 1 & 0\\ & \iddots & & \\ 0 & 1 & \cdots & 0\end{pmatrix} \quad (1)$$

The $k^{(\mathrm{th})}$ received blocks, $\forall\ k = 2i, 2i+1$, in the presence of noise is given by

$$\mathrm{y}(k) = \mathrm{H}_1(k)x_1(k) + \mathrm{H}_2(k)x_2(k) + \mathrm{n}(k) \quad (2)$$

where $\mathrm{n}(k)$ is the noise term which is assumed zero mean Gaussian with white power spectrum, and $\mathrm{H}_1(k)$ and $\mathrm{H}_2(k)$ are the circulant channel matrices from antenna one and two, respectively, to the receive antenna. This index implies that the channels are not assumed to be quasi-static. It should be noted that the original Toeplitz channel structure is converted to a circulant structure by the addition of the cyclic prefix of length L defined in (1). The circulant channel results from the addition of the cyclic prefix of length L.

Next, applying the $N \times N$ DFT matrix $\mathbf{F}_N$, to the received sequence we get

$$\mathrm{Y}(k) = \mathbf{F}_N \cdot \mathrm{y}(k) = \Lambda_1(k)\mathrm{X}_1(k) + \Lambda_2(k)\mathrm{X}_2(k) + \mathrm{N}(k) \quad (3)$$

where $\mathrm{X}(k) = \mathbf{F}_N \cdot x(k)$, $\mathrm{N}(k) = \mathbf{F}_N \cdot \mathrm{n}(k)$ and $\Lambda_1(k)$ and $\Lambda_2(k)$ are the diagonal matrices of $\mathrm{H}_1(k)$ and $\mathrm{H}_2(k)$, respectively. The $(i,k)^{th}$ element of the DFT matrix $\mathbf{F}_N$ is defined as

$$\left[\mathrm{F}_N\right]_{i,k} = \frac{1}{\sqrt{N}} e^{-j\frac{2\pi}{N}ik}, \quad j=\sqrt{-1},\ i,k = 1,2,\cdots,N-1 \quad (4)$$

Using the properties of DFT, the terms for the $2i+1$ block can be written as

$$\begin{aligned}\mathrm{X}_1(2i+1) &= -\mathrm{X}_2^*(2i)\\ \mathrm{X}_2(2i+1) &= \mathrm{X}_1^*(2i)\end{aligned} \quad (5)$$

Combining (3) and (5), we get

$$\mathbf{Y}=\begin{pmatrix}\mathrm{Y}(2i)\\ \mathrm{Y}^*(2i+1)\end{pmatrix}=\underbrace{\begin{pmatrix}\Lambda_1 & \Lambda_2\\ \Lambda_2^* & -\Lambda_1^*\end{pmatrix}}_{\text{quatrionic structure}}\cdot\begin{pmatrix}\mathrm{X}_1(2i)\\ \mathrm{X}_2(2i)\end{pmatrix}+\begin{pmatrix}\mathrm{N}(2i)\\ \mathrm{N}^*(2i+1)\end{pmatrix} \quad (6)$$

It should be noted that the choice of the permutation matrix (1) alleviates the need of post multiplying the received sequence by the $\mathbf{P}$ as in [5]. It is clear from the Alamouti-like diagonal channel matrix in (6) that by forming the unitary matrix ,

$$\Lambda^H = \begin{pmatrix}\Lambda_1 & \Lambda_2\\ \Lambda_2^* & -\Lambda_1^*\end{pmatrix}^H \quad (7)$$

The data sequence can be decoupled by the following unitary operation,

$$\tilde{\mathbf{Y}} = \Lambda^H\mathbf{Y}=\begin{pmatrix}\Lambda_0 & 0\\ 0 & \Lambda_0\end{pmatrix}\cdot\begin{pmatrix}\mathrm{X}_1(2i)\\ \mathrm{X}_2(2i+1)\end{pmatrix}+\tilde{\mathbf{W}} \quad (8)$$

where

$\Lambda_0 = (\Lambda_1\Lambda_1^* + \Lambda_2\Lambda_2^*)$ and $\tilde{\mathbf{W}}=\Lambda^H\left[\mathrm{N}(2i) \quad \mathrm{N}^*(2i+1)\right]^T$.

Next we define the minimum mean square estimator (MMSE) equalizer [7] as

$$\tilde{\Lambda} = \left(\Lambda^H\Lambda + \frac{1}{\mathrm{SNR}}\mathbf{I}_{2N}\right)^{-1} \quad (9)$$

The SNR at the receiver is given by $\mathrm{SNR}=\sigma_x^2/\sigma_w^2$, where σ_w is the covariance of noise, σ_x is the signal covariance. The MMSE estimate of X is then given as

$$\hat{\mathrm{X}}=\begin{bmatrix}\hat{\mathrm{X}}_1(2i)\\ \hat{\mathrm{X}}_2(2i)\end{bmatrix} = \tilde{\Lambda}\Lambda^H\mathbf{Y}=\left(\Lambda^H\Lambda + \frac{1}{\mathrm{SNR}}\mathbf{I}_{2N}\right)^{-1}\Lambda^H\mathbf{Y} \quad (10)$$

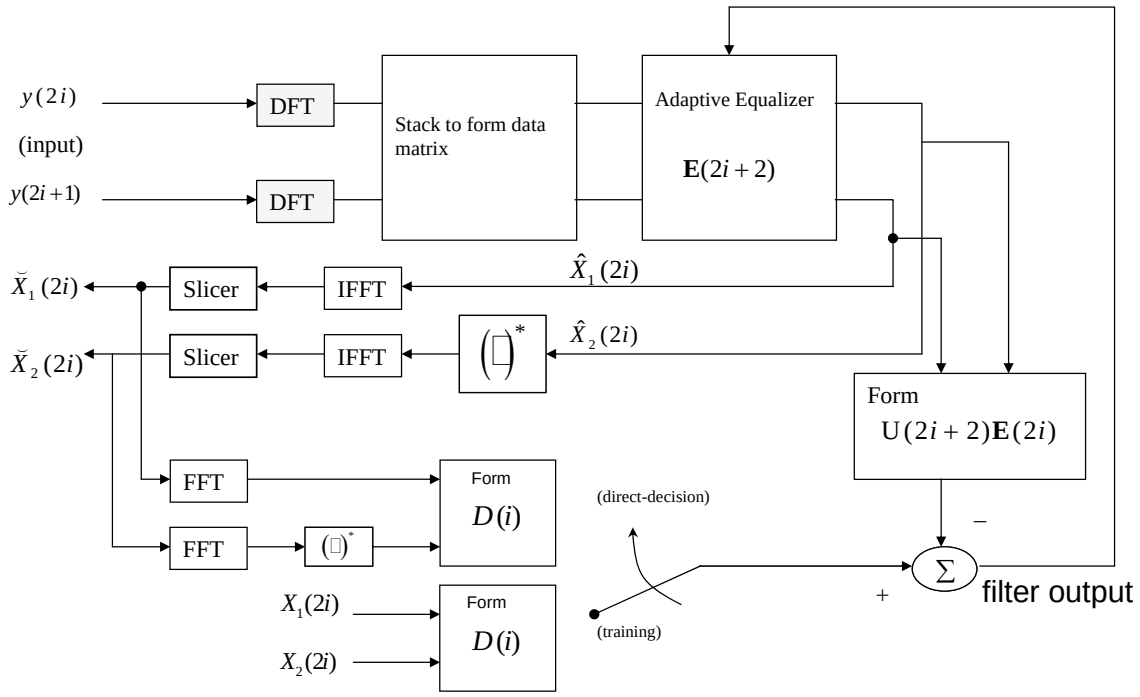

Fig. 1 Block diagram for the single user adaptive receiver with two-transmit one-receive antennas

2.2 Adaptive Implementation

The interference cancellation and equalization technique described in the previous section requires the knowledge of the channel state information (CSI) at the receiver. This is usually accomplished by the addition of a training (pilot) sequence to each transmitted block in order to estimate the channel at the expense of additional bandwidth requirement. In order to decrease the overhead requirements, such pilot aided schemes will require longer blocks which become impractical in channels with fast variations. Furthermore blind channel estimation based on second [20] and higher order statistics results in higher complexity at the receiver and is not suitable for online implementation.

Hence the need of an online adaptive receiver under such conditions becomes imperative. The RLS algorithm provides fast tracking , and due to the special quadtronic structure of space-time block codes, the complexity can be reduce to that of an LMS algorithm. The overall adaptive receiver is shown in Fig. 1.

Defining the combined matrix of the MMSE in (10) as $\mathbf{B} = \tilde{\Lambda}\Lambda^H$, it can be shown that this matrix has an Alamouti (quadtronic) structure i.e.

$$\mathbf{B}=\begin{pmatrix} \mathrm{B}_1 & \mathrm{B}_2 \\ \mathrm{B}_2^* & -\mathrm{B}_1^* \end{pmatrix} \tag{11}$$

where the entries of $\mathbf{B}$, given the block size N , are given by

$$\begin{aligned} \mathrm{B}_1 &= \mathrm{diag}\left\{ \frac{1}{\Lambda_0(n,n)+1/\mathrm{SNR}} \right\}_{n=0}^{N-1} \cdot \Lambda_1^* \\ \mathrm{B}_2 &= \mathrm{diag}\left\{ \frac{1}{\Lambda_0(n,n)+1/\mathrm{SNR}} \right\}_{n=0}^{N-1} \cdot \Lambda_2 \end{aligned} \tag{12}$$

Hence (10) can be written as

$$\begin{pmatrix} \hat{\mathrm{X}}_1(2i) \\ \hat{\mathrm{X}}_2(2i) \end{pmatrix} = \begin{pmatrix} \mathrm{B}_1 & \mathrm{B}_2 \\ \mathrm{B}_2^* & -\mathrm{B}_1^* \end{pmatrix} \mathbf{Y} \tag{13}$$

This can be rearranged into the following form.

$$\begin{pmatrix} \hat{\mathrm{X}}_1(2i) \\ \hat{\mathrm{X}}_2^*(2i) \end{pmatrix} = \underbrace{\begin{pmatrix} \mathrm{diag}(\mathrm{Y}(2i)) & \mathrm{diag}(\mathrm{Y}^*(2i+1)) \\ -\mathrm{diag}(\mathrm{Y}(2i+1)) & \mathrm{diag}(\mathrm{Y}^*(2i)) \end{pmatrix}}_{\text{quadtronic structure}} \cdot \begin{pmatrix} \mathrm{E}_1 \\ \mathrm{E}_2 \end{pmatrix} = \mathrm{U}(i)\mathbf{E} \tag{14}$$

The vectors E_1 and E_2 contain the diagonal entries of B_1 and B_2 , respectively. The essence of this derivation lies in the manner in which the quadtronic structure is maintained in (14), which is in the form of the RLS problem [12-13]. The adaptive RLS solution is now applied. The equalizer coefficients $\mathbf{E}$ are adaptively updated for every two blocks using the following recursion [15]:

$$\begin{aligned} &\mathbf{E}(2i+2) \\ &= \mathbf{E}(2i) + Q(2i+2)\mathrm{U}^H(2i+2)\left[\mathrm{D}(2i+2) - \mathrm{U}(2i+2)\mathbf{E}(2i)\right] \end{aligned} \tag{15}$$

where

$$\begin{aligned} &Q(2i+2) = \lambda^{-1}[Q(2i) - \lambda^{-1}Q(2i)\mathrm{U}(2i+2) \\ &\times\left(\mathrm{I}_{2N} + \lambda^{-1}\mathrm{U}(2i+2)Q(2i)\mathrm{U}^H(2i+2)\right)^{-1}\mathrm{U}^H(2i+2)Q(2i)] \end{aligned} \tag{16}$$

It is easy to see that the inverse term in (16) is given by a diagonal matrix

$$\left(\mathrm{I}_{2N}+\lambda^{-1}\mathrm{U}(2i+2)Q(2i)\mathrm{U}^{H}(2i+2)\right)^{-1}=\begin{pmatrix}\Theta(2i+2) & 0\\ 0 & \Theta(2i+2)\end{pmatrix} \quad (17)$$

$\mathrm{D}(2i+2)$ in (15) is referred to as the desired response and is given by

$$\mathrm{D}(2i+2)=\begin{cases}\begin{pmatrix}\mathrm{X}_1(2i+2)\\ \mathrm{X}_2^{*}(2i+2)\end{pmatrix}, \text{for training}\\ \begin{pmatrix}\breve{\mathrm{X}}_1(2i+2)\\ \breve{\mathrm{X}}_2^{*}(2i+2)\end{pmatrix}, \text{for decision-direct tracking.}\end{cases} \quad (18)$$

The parameters of the algorithm are initialized as follows: $\mathbf{E}(0)=0$ and $Q(0)=\delta\mathrm{I}_{2N}$, with δ being a large number (usually $\approx 10^{6}$ [18]). λ is called the forgetting factor and is in the range $[0,1]$.

The adaptive receiver operates in two modes. $\left[\mathrm{X}_1(2i+2)\quad \mathrm{X}_2^{*}(2i+2)\right]^{T}$ denotes the pilot block during training mode and $\left[\breve{\mathrm{X}}_1(2i+2)\quad \breve{\mathrm{X}}_2^{*}(2i+2)\right]^{T}$ denotes the slicer output of the received data during the decision direct mode as shown in Fig. 1.

$Q(2i+2)$ has the following diagonal structure.

$$Q(2i+2)=\begin{pmatrix}T(2i+2) & 0\\ 0 & T(2i+2)\end{pmatrix} \quad (19)$$

The recursive updates of $T(2i+2)$ is given by

$$T(2i+2)=\lambda^{-1}\left(T(2i)-\lambda^{-1}T(2i)\Omega(2i+2)T(2i)\right) \quad (20)$$

where

$$\Omega(2i+2)=\Theta(2i+2)\mathrm{diag}\left(\left|\mathrm{Y}(2i)\right|^{2}+\left|\mathrm{Y}(2i+1)\right|^{2}\right) \quad (21)$$

The diagonal matrix $\Theta(2i+2)$ in (17) is given by

$$\Theta(2i+2)=\left(\mathrm{I}_{N}+\lambda^{-1}T(2i)\mathrm{diag}\left(\left|Y(2i)\right|^{2}+\left|Y(2i+1)\right|^{2}\right)\right)^{-1} \quad (22)$$

Hence we get

$$\Omega(2i+2)=\left[\mathrm{diag}\left(\left|\mathrm{Y}(2i)\right|^{2}+\left|\mathrm{Y}(2i+1)\right|^{2}\right)^{-1}+\lambda^{-1}T(2i)\right]^{-1} \quad (23)$$

Finally the RLS equalizer is then given by

$$\mathbf{E}(2i+2)=\mathbf{E}(2i)+\begin{pmatrix}T(2i+2) & 0\\ 0 & T(2i+2)\end{pmatrix}\mathrm{U}^{H}(2i+2) \quad (24)$$
$$\times\left[\mathrm{D}(2i+2)-\mathrm{U}(2i+2)\mathbf{E}(2i)\right].$$

At first glance the RLS algorithm may appear computationally complex, due to the number of matrix inversions required in the algorithm. However, due to quadtronic structure of $\mathrm{Y}(i)$ and the diagonal structure of $T(i)$, the matrix inversions in (22) and (23) are in fact scalar inversions. This results in the algorithm giving an LMS complexity. We will now describe a new method of decreasing the need of an entire pilot block during training mode as shown in (18). The solution is based on the forward LP and the knowledge of the autocorrelation function for the broadband channel.

3. LINEAR PREDICTION ALGORITHM

3.1 Continuous Time Channel Model

The received signal for the Rayleigh frequency-flat fading channel is modelled as [21]:

$$r_c(t)=\mathrm{Re}\left\{v(t)h(t)\sqrt{2}\exp\{j2\pi f_c t\}\right\}+n_c(t) \quad (25)$$

where $v(t)$ is the transmitted baseband signal, $n_c(t)$ is the AWGN noise, $h(t)$ is the continuous-time fading process and f_c is the frequency of the fading process. The fading process is modelled as a zero-mean, wide-sense stationary, complex Guassian random process. The amplitude $|h(t)|$ has a Rayleigh distribution. The phase of the fading process, which represents the carrier phase error, is uniformly distributed over $[0,2\pi)$. The fading process is a time variant process which makes the fading estimation problem a difficult one. Added to this is the fact that the amplitude, $|h(t)|$, can have a small value for extended periods of time (this represents a deep fade). Assuming the fading process is correlated in time, the autocorrelation function is given as:

$$\phi_F(\Delta t)=\frac{1}{2}\mathbf{E}\left[h^{*}(t-\Delta t)h(t)\right] \quad (26)$$

A commonly used model to represent the land mobile fading process is the Jakes model [17]. The autocorrelation function for this model is given as:

$$\phi_F(\Delta t)=\frac{1}{2}J_0(2\pi B_d\Delta t) \quad (27)$$

where $J_0(\cdot)$ is the order zero Bessel function of the first kind, and B_d is the Doppler spread of the channel. We assume that the channel follows the Rayleigh fading model with the autocorrelation function given by (27). Next, we use the LP to decrease the pilot requirements for the RLS equalizer.

3.2 Applying Linear Prediction to the RLS Algorithm

The M^{th}-order linear forward predictor for the channel coefficients is given by [21]:

$$\hat{h}_m = \frac{1}{\varepsilon_s}\sum_{m=0}^{M-1} c_m^* h_{m-1} \tag{28}$$

where $\hat{h}_m$ are the channel coefficients and c_m are the predictor coefficients. The predictor coefficients are the solution to the Wiener-Hopf equation [19] given by:

$$\begin{bmatrix} \varepsilon_s\phi_F(0) & \varepsilon_s\phi_F(1) & \cdots & \varepsilon_s\phi_F(M-1) \\ \varepsilon_s\phi_F(1) & \varepsilon_s\phi_F(0) & \cdots & \varepsilon_s\phi_F(M-2) \\ \vdots & \vdots & \ddots & \vdots \\ \varepsilon_s\phi_F(M-1) & \varepsilon_s\phi_F(M-2) & \cdots & \varepsilon_s\phi_F(0) \end{bmatrix} \cdot \begin{bmatrix} c_0 \\ c_1 \\ \vdots \\ c_{M-1} \end{bmatrix} = \begin{bmatrix} \varepsilon_s\phi_F(M) \\ \varepsilon_s\phi_F(M-1) \\ \vdots \\ \varepsilon_s\phi_F(1) \end{bmatrix} \tag{29}$$

where ε_s is the normalized energy for the channel and $\phi_F(m)$ is as defined in (27). The size of the window must be at-least greater than or equal to the length of the channel. For each given tap, we need to get $L+1$ previous values, where L is the length of the channel. Hence we send a pilot sequence of at least length $L+1$. We will once again use the example of two antennas and one receive antenna. Let the channel circulant matrix be given by:

$$\mathrm{H}_\mu = \begin{bmatrix} h_{0,\mu} & \cdots & h_{L-1,\mu} & h_{L,\mu} & \cdots & 0 \\ 0 & \ddots & \ddots & h_{L-1,\mu} & h_{L,\mu} & \vdots \\ \cdots & \cdots & h_{0,\mu} & \cdots & \cdots & h_{L,\mu} \\ h_{L,\mu} & h_{L-1,\mu} & \cdots & h_{0,\mu} & 0 & h_{L-1,\mu} \\ \vdots & \ddots & \ddots & \ddots & \ddots & \vdots \\ h_{1,\mu} & \cdots & h_{L,\mu} & h_{L-1,\mu} & \cdots & h_{0,\mu} \end{bmatrix} \quad \forall\ \mu = 1, 2, \tag{30}$$

in terms of the channel impulse response sequence $h_\mu \square \left[h_{0,\mu},\ h_{1,\mu},\ \cdots,\ h_{L,\mu}\right]$, where H_μ is an $R \times R$ circulant matrix if R samples of the received sequence are taken into account. The index, μ, represents the two different paths. It should be noted that the original Toeplitz channel structure is converted to a circulant structure by the addition of the cyclic prefix of length L defined in (1). The circulant channel results from the addition of the cyclic prefix of length L.

Let $\tilde{x}_1 = x_1^T$, $x_2 = x_2^T$, $\tilde{H}_1 = H_1^T$, $\tilde{H}_2 = H_2^T$, $\tilde{Y}_1 = Y_1^T$ and $\tilde{Y}_2 = Y_2^T$. The received sequence given in (2) can be re-written as

$$\tilde{\mathrm{Y}} = \begin{bmatrix} \tilde{\mathrm{Y}}_1 \\ \tilde{\mathrm{Y}}_2 \end{bmatrix} = \underbrace{\begin{bmatrix} \tilde{x}_1 & \tilde{x}_2 \\ -\mathbf{P}\tilde{x}_2^* & \mathbf{P}\tilde{x}_1^* \end{bmatrix}}_{\tilde{\mathrm{X}}} \underbrace{\begin{bmatrix} \tilde{\mathrm{H}}_1 \\ \tilde{\mathrm{H}}_2 \end{bmatrix}}_{\tilde{\mathrm{H}}} + \begin{bmatrix} n_1 \\ n_2 \end{bmatrix} \tag{31}$$

where the size of $\tilde{Y}_1$, $\tilde{Y}_2$, $\tilde{x}_1$, $\tilde{x}_2$, n_1 and n_2 is $1 \times R$.

In training mode, the algorithm proceeds as follows. Ignoring the noise components we get

$$\tilde{\mathrm{Y}} = \tilde{\mathrm{X}} \cdot \tilde{\mathrm{H}} \tag{32}$$

where $\tilde{\mathrm{X}}$ and $\tilde{\mathrm{H}}$ are as defined in (31). Since the pilot sequence is known, the matrix $\tilde{\mathrm{X}}$ is reconstructed at the receiver. The length of the pilot sequence corresponds to the window size of the LP. If the channel length is given by L, then $M > L$. The zero forcing (ZF) solution for the two channels is given by [6]:

$$\tilde{\mathrm{H}} = \begin{bmatrix} \tilde{\mathrm{H}}_1 \\ \tilde{\mathrm{H}}_2 \end{bmatrix} = \left(\tilde{\mathrm{X}}^H \cdot \tilde{\mathrm{X}}\right)^{-1} \cdot \left(\tilde{\mathrm{X}}^H\right) \cdot \tilde{\mathrm{Y}} \tag{33}$$

It must be noted, that there is no DFT and IDFT operations in the training period just described. Hence, the tap components required for the initial window of the linear estimator are retrieved. The algorithm then switches to direct-decision mode which has the DFT and IDFT operations. We define the diagonal matrices as

$$\begin{aligned} \Lambda_1 &= \mathrm{F}_N\, \tilde{\mathrm{H}}_1\, \mathrm{F}_N^*, \\ \Lambda_2 &= \mathrm{F}_N\, \tilde{\mathrm{H}}_2\, \mathrm{F}_N^*, \\ \Lambda_0 &= (\Lambda_1\Lambda_1^* + \Lambda_2\Lambda_2^*) \end{aligned} \tag{34}$$

where $\tilde{\mathrm{H}}_1$ and $\tilde{\mathrm{H}}_2$ represent circulant channel matrices. The tap values, and hence the circulant matrices $\tilde{\mathrm{H}}_1$ and $\tilde{\mathrm{H}}_2$, are then estimated for the next block using (28), with the predictor coefficients for the previous window of size M already defined from the training period. The diagonal matrices are then derived using (34).

Using (11), we can solve for the channel matrix entries B_1 and B_2, and hence solve for the channel vector E in (15). To summarize, the algorithm is implemented as follows:

1. The shortened pilot stream is sent and using $\tilde{\mathrm{H}} = \begin{bmatrix} \tilde{\mathrm{H}}_1 & \tilde{\mathrm{H}}_2 \end{bmatrix}^T = \left(\tilde{\mathrm{X}}^H \cdot \tilde{\mathrm{X}}\right)^{-1} \cdot \left(\tilde{\mathrm{X}}^H\right) \cdot \tilde{\mathrm{Y}}$ the initial estimates of the channel taps are updated.

2. The LP then estimates the channel coefficients for the next block using (28). Hence we update $\tilde{\mathrm{H}}_1$ and $\tilde{\mathrm{H}}_2$.

3. By solving Λ_0 in (34) and B_1 and B_2 in (11), the vector channel vector, E in (15), is updated. The values of $\Omega(i)$ and $T(i)$ in (23) and (20), respectively, are then updated.

4. The RLS algorithm then switches to direct-decision mode, until it is re-trained again.

The pilot requirement for the system is therefore decreased to the predefined window size M. This key result improves the system performance in the following two ways:

- Given that the addition of the linear prediction algorithm does not depreciate the system performance in terms of frame error rate (FER), the resultant system has a greater throughput than the system without linear prediction. This is because, although the FER for the new system is

the same as the old system, the decrease in number of pilot symbols required increases the overall data sent. Hence there is an improvement in performance in terms of bandwidth efficiency.

- In [15] it is shown that by decreasing the re-training interval for an adaptive algorithm, the overall performance in terms of FER improves. The reduction in the number of pilot symbol requirements in the linear prediction system allows the re-training interval to be decreased while still using the same bandwidth as the old system. Hence the overall system performance in terms of FER can be improved by sacrificing some of the bandwidth efficiency gained using linear prediction.

It is also mentioned in [15] that the RLS algorithm suffers in terms robustness particularly at higher Doppler frequencies. To achieve better robustness at higher Doppler frequencies, an adaptive QRD based receiver is derived in the next section.

4. MODIFIED QRD BASED RECEIVER

4.1 QRD receiver

The QR solution to the least squares problem is documented in [19]. In order to apply the algorithm to our receiver, we recall from (14) that the least squares problem is given by

$$\begin{pmatrix} \hat{\mathrm{X}}_1(2i) \\ \hat{\mathrm{X}}_2^*(2i) \end{pmatrix} = \underbrace{\begin{pmatrix} \mathrm{diag}(\mathrm{Y}(2i)) & \mathrm{diag}(\mathrm{Y}^*(2i+1)) \\ -\mathrm{diag}(\mathrm{Y}(2i+1)) & \mathrm{diag}(\mathrm{Y}^*(2i)) \end{pmatrix}}_{\text{Quadtronic structure}} \cdot \begin{pmatrix} \mathrm{E}_1 \\ \mathrm{E}_2 \end{pmatrix} = \mathrm{U}(i)\mathbf{E} \quad (35)$$

where $\mathbf{E} = \begin{bmatrix} \mathrm{E}_1 & \mathrm{E}_2 \end{bmatrix}^T$ is the effective channel coefficient vector after the FFT operation and $\mathrm{U}(i)$ is the received observation sequence. Once again we define the desired response as

$$\mathrm{D}(2i+2) = \begin{cases} \begin{pmatrix} \mathrm{X}_1(2i+2) \\ \mathrm{X}_2^*(2i+2) \end{pmatrix}, \text{for training} \\ \begin{pmatrix} \breve{\mathrm{X}}_1(2i+2) \\ \breve{\mathrm{X}}_2^*(2i+2) \end{pmatrix}, \text{for direct-decision tracking} \end{cases} \quad (36)$$

The algorithm proceeds with the following four steps:

1. The channel response vector, $\mathbf{E}$, is initialized to zero.

2. Perform QR decomposition of the U received sequence matrix in (35). Hence we get
$Q(2i+2)R(2i+2) = \mathrm{U}(2i+2)$

   which is computed using the Givens rotation described in [19].

3. The error signal is computed as
$\mathbf{P}(2i+2) = \left[\mathrm{D}(2i+2) - \mathrm{U}(2i+2)\mathbf{E}(2i)\right]$

4. Finally, the recursive update is given as
$\mathbf{E}(2i+2)$
$= \mathbf{E}(2i) + R(2i+2)^{-1}Q(2i+2)\mathbf{P}(2i+2)$

The overall block diagram for the QRD based receiver is shown in Fig. 2. The only modification to the receiver block diagram of Fig 1 is the addition of the QRD block. In the next subsection, the LP is added to the QR-based receiver in order to shorten the pilot requirement for the system.

4.2 QRD receiver with LP

To incorporate the LP, we pursue the exact same steps we described in section 3. Using (26)-(34), we estimate the initial values for the channel vector $\mathbf{E}$. The algorithm then switches to direct-decision mode and the values of $\mathbf{E}$ are then updated recursively using (37), (38) and (39).

1. The shortened pilot stream is sent, and using $\tilde{\mathrm{H}} = \begin{bmatrix} \tilde{\mathrm{H}}_1 & \tilde{\mathrm{H}}_2 \end{bmatrix}^T = \left(\tilde{\mathrm{X}}^H \cdot \tilde{\mathrm{X}}\right)^{-1} \cdot \left(\tilde{\mathrm{X}}^H\right) \cdot \tilde{\mathrm{Y}}$ the initial estimates of the channel taps are updated.

2. The LP then estimates the channel coefficients for the next block using (28). Hence we update $\tilde{\mathrm{H}}_1$ and $\tilde{\mathrm{H}}_2$.

3. By solving Λ_0 in (8) and B_1 and B_2 in (11), the vector channel vector, $\mathbf{E}$ in (15), is updated. The values of $\Omega(i)$ and $T(i)$ in (23) and (20), respectively, are then updated.

4. The error signal is computed as $\mathbf{P}(2i+2) = \left[\mathrm{D}(2i+2) - \mathrm{U}(2i+2)\mathbf{E}(2i)\right]$

5. Finally, the recursive update is given as $\mathbf{E}(2i+2) = \mathbf{E}(2i) + R(2i+2)^{-1}Q(2i+2)\mathbf{P}(2i+2)$

The overall block diagram for the QRD-based receiver with linear prediction (QRD-LP) is shown in Fig 2.

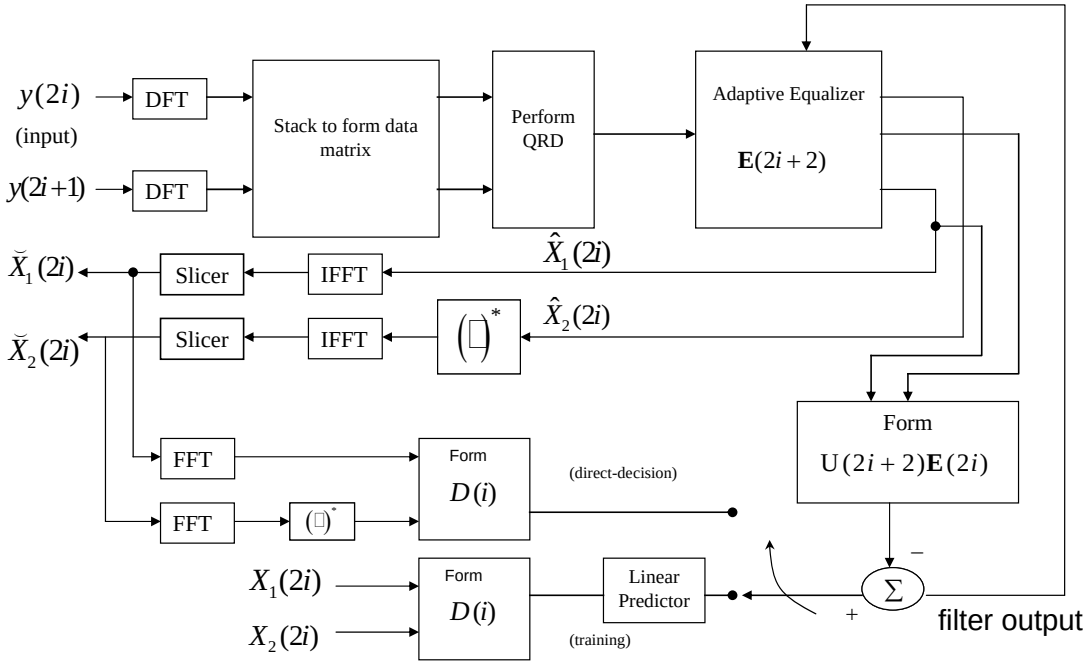

Fig. 2 Equivalent receiver model with the QRD and LP

Table 1 A typical urban (TU) channel model

Delay (μsec)	0.0	0.2	0.5	1.6	2.3	5.0
Strength (dB)	-3.0	0.0	-2.0	-6.0	-8.0	-10

5. SIMULATION RESULTS

We now present the simulation results for the modified RLS algorithm that includes the LP. The main objective of the simulations is to verify that there is no significant performance loss incurred by using the LP. Provided that there is no performance loss, we are able to increase the re-training interval while still maintaining the same effective number of pilot symbols. This is once again shown in the simulation results.

Computer simulations are also carried out to compare the performance of the QRD and RLS algorithms with respect to the tracking (non-stationary) and steady state (stationary) performance. We then verify through simulations that there is no significant performance loss when combining QRD based receiver with the LP. Finally, we show results of the new QRD-LP receiver and compare this to the RLS receiver in [16]. These results summarize our achievements by showing how the new QRD-LP receiver outperforms the RLS receiver in terms of bandwidth efficiency and robustness at higher Doppler frequencies.

5.1 Simulation Environment

The enhanced data rate for global evolution (EDGE) simulation environment is used to test the performance of this adaptive receiver. The EDGE typical urban (TU) channel with 8-PSK modulation is considered. Equalization for EDGE poses a challenging problem due to the use of 8-PSK modulation unlike its predecessor that uses binary modulation in GSM. The TU channel impulse response generally has a non-minimum phase characteristic and the guassian minimum shift keying (GMSK) transmit filter used to combat this adds additional ISI. The delay profile of the TU channel is presented in Table 1 [15, 16].

The symbol duration of $T_s = 3.69\ \mu$s and $\sigma = 0.3$ is proposed in 3rd generation TDMA cellular standard EDGE (2.5G). The overall TU channel impulse response (CIR) after GMSK pulse shaping is given is Fig. 3.

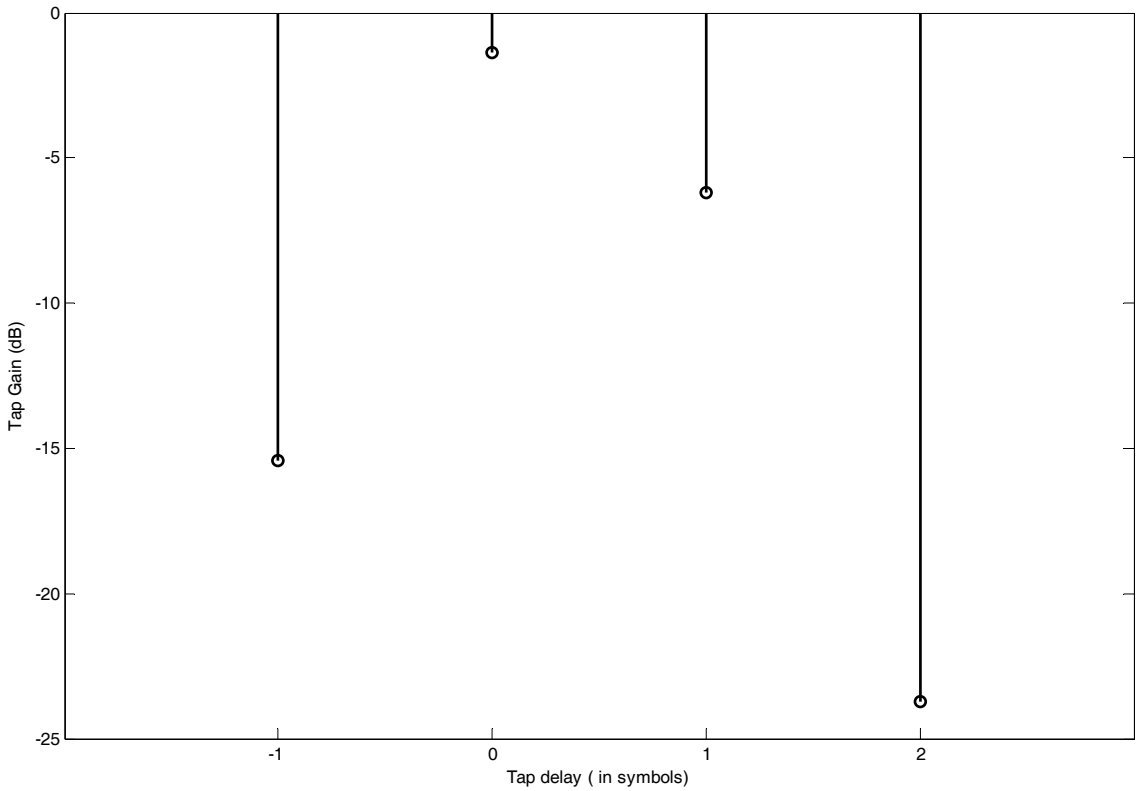

Fig. 3 Equivalent CIR for a TU channel with GMSK pulse shaping.

From Fig. 3, the overall channel has a length of four symbols and hence the channel memory is $L = 3$. All channels are assumed independent. The performance of the RLS algorithm is shown for different frequencies. The Jakes model is used to generate the Rayleigh fading coefficients. All taps are assumed independent and identically distributed (i.i.d.) Gaussian.

Next, we present the simulation results for the modified RLS algorithm that includes the LP. The main objective of the simulations is to verify that there is no significant performance loss incurred by using the LP. Provided that there is no performance loss, we are able to increase the re-training interval while still maintaining the same effective number of pilot symbols. This is once again verified in the simulation results.

5.2 New Linear Prediction Based RLS Receiver

5.2.1 Performance Penalty

The initial set of simulation results are done to investigate if there is any performance loss incurred by using the new linear prediction based algorithm. The original RLS receiver is set with frequencies of 10 Hz and 40 Hz. The block size of 32 symbols is used. The re-training interval is set to 50 blocks in all cases and the window size of the LP, M, is set to 10 blocks. The new receiver with the LP is also set with the same frequencies and re-training interval.

Fig. 4 shows that the performance penalty incurred is negligible, hence making this an attractive method of improving the overall performance of the adaptive receiver. The auto-correlation function in (27) is an accurate model for the Rayleigh fading process used. It is shown in [19] that the forward LP performance is dependant on the accuracy of the auto-correlation function. This is the reason for the performance penalty being minimal.

5.2.2 Performance Using Equivalent Pilot Symbols

The LP decreases the overhead required by the system during the training period of the algorithm. Fig. 5 shows the RLS algorithm with the training period that requires an entire block of pilot symbols as compared to the new receiver with linear prediction that shortens this requirement. The block size of 40 symbols and Doppler frequency of 40Hz are used. The re-training

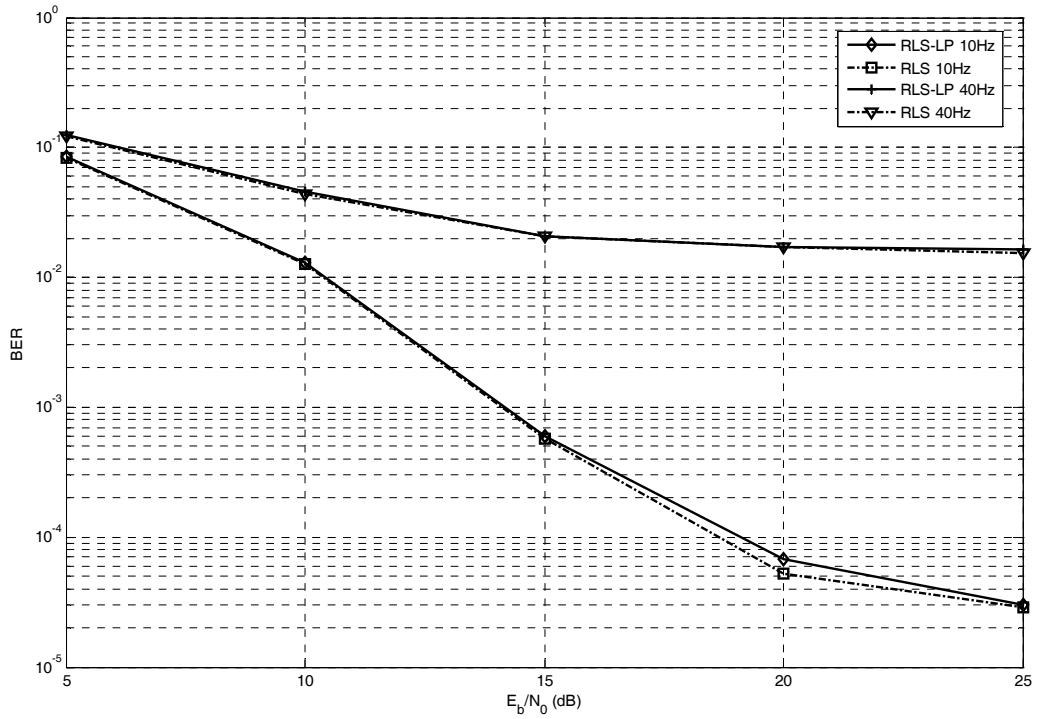

Fig. 4 Comparison of performance penalty with the linear predictor

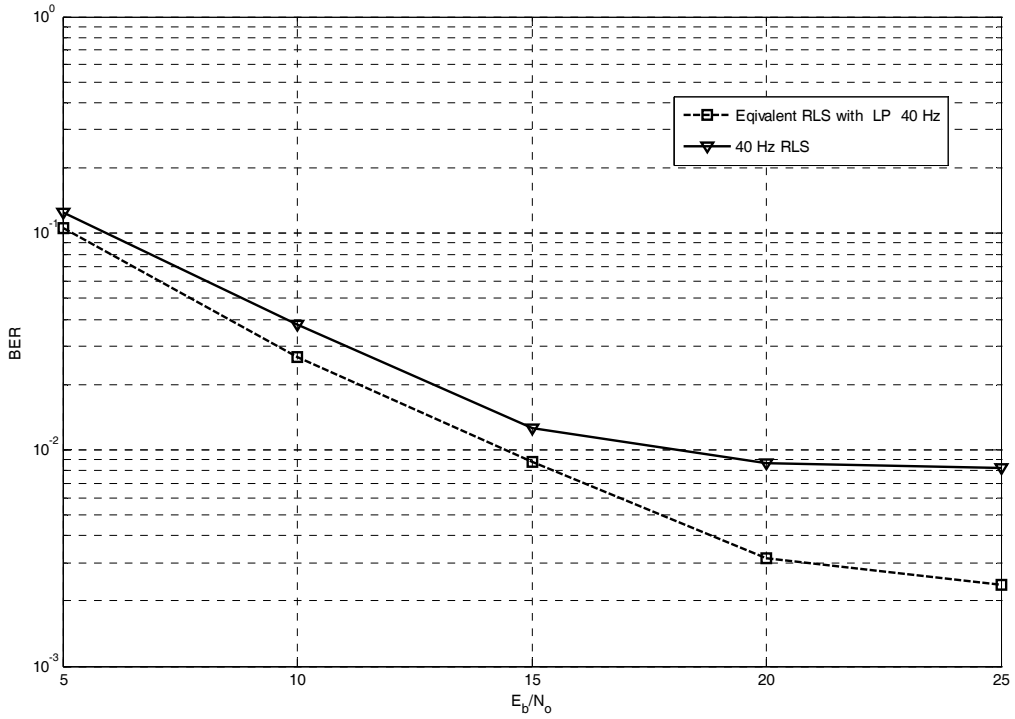

Fig 5 Performance of the linear predictor with equivalent number of pilot symbols.

interval is set to 40 blocks. The window size for the LP is set to 10. In order to use the equivalent number of pilot symbols, the re-training interval is decreased to 10 blocks for the new system. From [16], it was concluded that increasing the retraining interval increases the overall system performance. Therefore, using the LP improves the performance of the adaptive receiver without the additional bandwidth requirement. From these results, an adjustment to the window size for the LP can result in better performance as the re-training interval can be decreased further. Since $M > L$, the knowledge of the channel length is required for this as it limits the window size that can be used.

5.3 QR Based Adaptive Receiver with Linear Prediction

The main purpose in this section is to investigate the following:

- Performance at high Doppler frequencies.
- Tracking and estimation error performance.
- Performance of the QR receiver with linear prediction.

5.3.1 Performance at High Doppler frequency

The main problem associated with the RLS algorithm is its lack of robustness, particularly at high Doppler frequencies. To achieve better performance at higher Doppler frequencies, an adaptive QRD based receiver was derived in section 4.

The result of computer simulation for the new QRD receiver is shown in Fig.6. The robustness of the new receiver as compared to the RLS based receiver is evident from the results in Fig. 6. The Doppler frequency of 100 Hz is used. The block size and re-training interval is set to 96 bits and 50 blocks, respectively.

Hence, by using the orthogonal transformation, the extent to which the ill-conditioned problem affects the estimates is reduced and hence the overall performance at high user mobility is improved.

5.3.2 Tracking and Estimation Error Performance

The purpose of this sub-section is to compare the tracking error and estimation error performance as the Doppler frequency is varied.

Fig. 7 shows the results at Doppler frequencies of 60 Hz, 40Hz and 0 Hz. We choose 60 Hz and 40 Hz to compare the tracking performance of the two algorithms at lower frequencies. The result at 0 Hz can be used to compare the estimation error performance of the two algorithms. The block size and re-training interval is set to 96 bits and 50 blocks, respectively.

The QRD based receiver provides a more robust solution as shown in the results for the Doppler frequencies of 60 Hz and 40 Hz. The results imply that the QR based solution has a better lag error or tracking performance than the RLS based receiver. The results at 0 Hz for both algorithms also show that the estimation error or steady state performance of the RLS algorithm is better than that of the QR based algorithm.

The RLS algorithm provides a better steady state performance. Since there are no transformations involved in this algorithm, the estimate error for the RLS algorithm in a stationary environment is more accurate than the QRD based approach. This is shown in Fig 7 for the Doppler frequency of 0 Hz where the RLS algorithm outperforms the QRD based receiver.

In order to further improve the performance of the receiver, the LP is combined with the QR based algorithm. The performance improvement can be achieved in terms of bandwidth efficiency and overall FER performance.

The next sub-section presents the simulation results that show these two performance improvements.

5.3.3 Performance of the QRD-LP

For the first set of simulations, the block size is set to 96 bits. The Doppler frequency of 60 Hz is used. The re-training interval is set to 50 blocks. The channel model and signal constellation is the same as previous section. The results in Fig. 8 shows that the addition of LP doesn't affect or hamper the performance to a significant extend. This emphasizes that the LP is an attractive method to shorten the preamble system requirements.

In order to verify this, we compare the QR receiver with fixed pilot symbols, and the QR-LP receiver with equivalent number of fixed pilot symbols.

For the second set of computer simulations in Fig. 9, the block size and Doppler frequency is set to 120 bits and 60 Hz, respectively. The re-training interval is set to 40 blocks for the RLS and QR algorithms. The window size for the LP is set to 40 bits and hence the equivalent re-training interval for the QR-LP is set to 10 blocks.

As opposed to its RLS predecessor, the new QR based receiver provides a more robust solution at higher frequencies. Combining the LP with the QRD based receiver results in decreasing the preamble requirements. This in-turn allows the system re-training interval to be decreased, hence increasing the overall receiver performance as shown in Fig.9. Hence

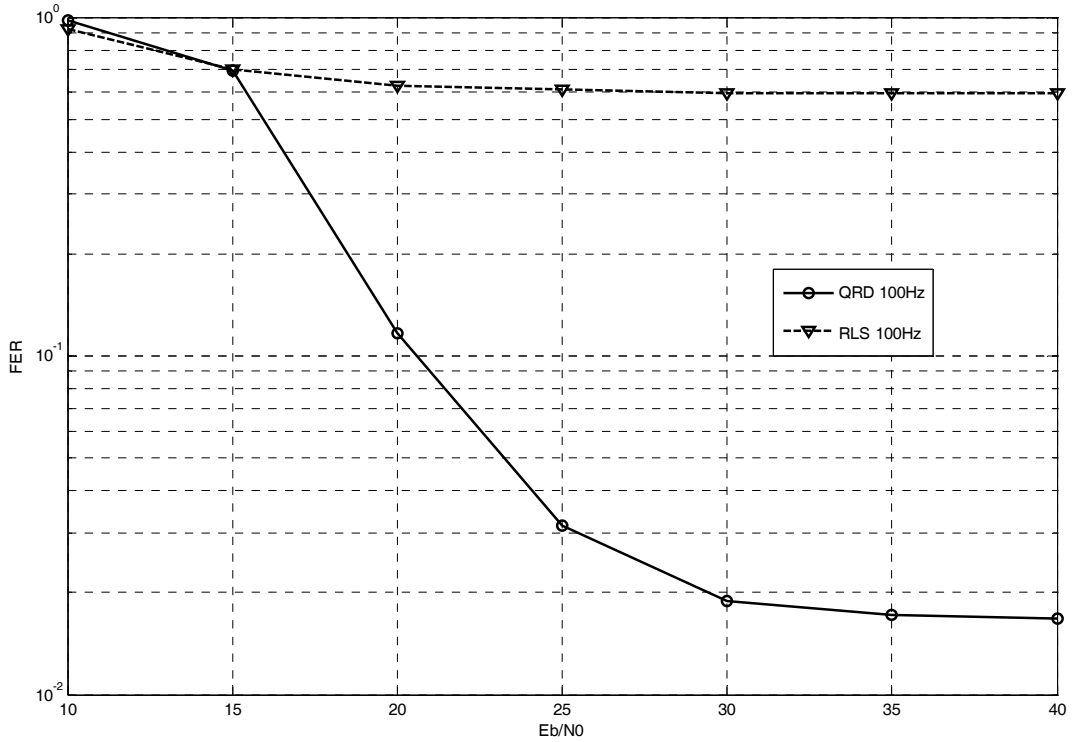

Fig 6 Simulation results to verify the robust property of the QRD algorithm

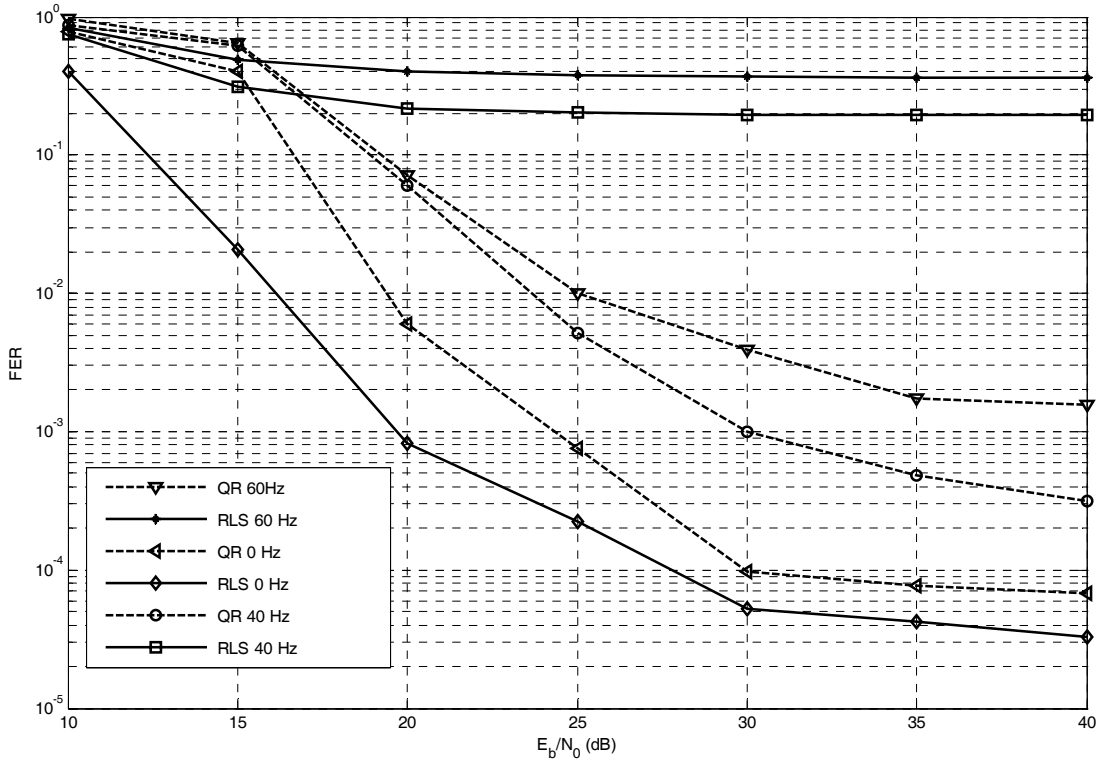

Fig 7 Simulation results of the QRD and RLS algorithms for different Doppler frequencies

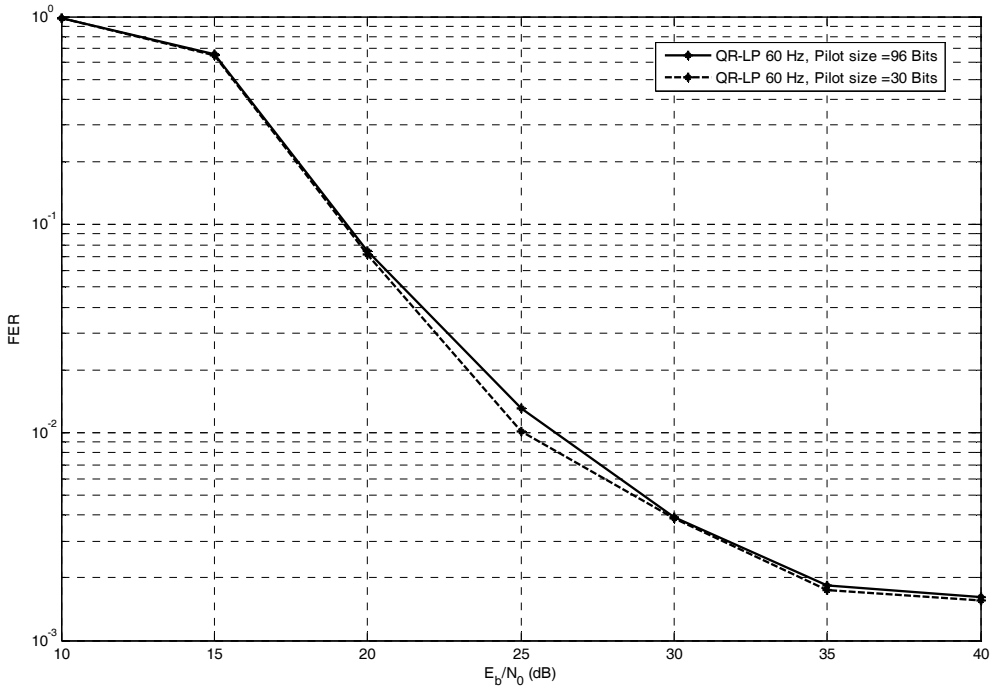

Fig 8 Comparison of QRD and QRD with LP at 60 Hz

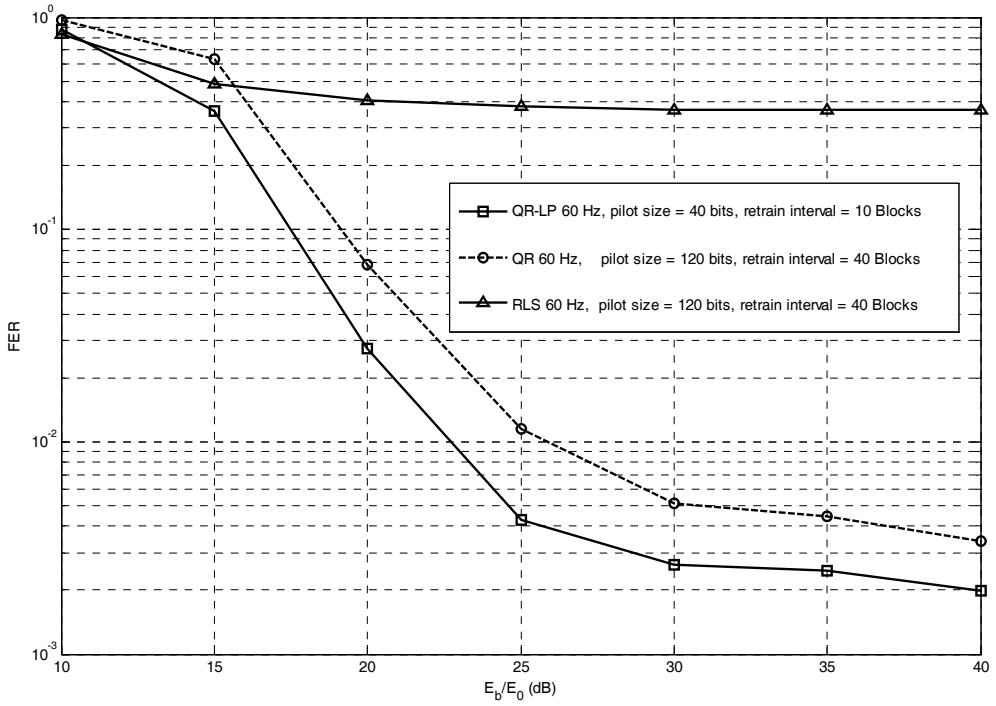

Fig 9 Overall modified QRD-LP receiver versus RLS receiver.

the results show a performance improvement for the new QRD-LP receiver when compared to its RLS counterpart.

6. CONCLUSION

We have described a bandwidth efficient method of improving the overall system performance of the adaptive RLS receiver. The LP decreases the number of pilot symbols that are required during the re-training period. Hence, the re-training interval can be decreased which results in the improved performance. The simulation results also show that there is no additional penalty when using the LP making it an attractive scheme. The only requirement at the receiver is that the knowledge of the autocorrelation function for the channel is assumed.

For the RLS based receiver in [15], the performance penalty at higher Doppler frequencies is larger when compared to the performance at lower frequencies. Hence, in this paper, we provide a more robust alternative algorithm for the adaptive receiver in [15] to perform joint interference and equalization at high Doppler frequencies. This is achieved by using a new algorithm based on QR orthogonal transformation.

Finally, the QRD based receiver is combined with the LP to increase the overall system performance by decreasing the re-training interval of the adaptive algorithm. This results in a receiver that offers stable performance at high frequencies and better overall performance as opposed to its RLS counterpart.

While the RLS based receiver provides an approach that does not require CSI estimation and hence reduces system overhead, the new QRD-LP based receiver provides a more robust solution while further decreasing the overhead requirements. The simulation results provide verification of the better performance for this new receiver.

7. REFERENCES

[1] S. M. Alamouti, “A simple transmit diversity technique for wireless communications,” *IEEE Journal on Selected Areas in Communications*, vol. 16, no. 8, pp.744-765, Aug. 1998.

[2] V. Tarokh, N. Seshadri, and A. R. Calderbank, “Space-time codes for high data rate wireless communication: performance criterion and code construction,” *IEEE Trans. on Information Theory*, vol. 44, no. 2, pp. 744-765, Feb. 1998.

[3] E. Lindskog and A. Paulraj, “A transmit diversity scheme for channels with inter-symbol interference,” *Proceedings of IEEE Conference on International Communications*, vol. 1, pp. 307-311, New Orleans, La, USA, June 2000.

[4] Z. Lui and G. B. Gannakis, “Space time block coded multiple access through frequency selective fading channels,” *IEEE Trans. Communications*, vol. 49, no. 6, pp.1033-1044, June 2001.

[5] S. Zhou and G. B. Giannakis, “Space-time coding with maximum diversity gains over frequency-selective fading channels,” *IEEE Signal Processing Letters*, vol. 8, no. 10, pp. 269-272, Oct. 2001.

[6] S. Zhou and G. B. Giannakis, “Single-carrier space-time block coded transmissions over frequency-selective fading channels,” *IEEE Trans. on Information Theory*, vol. 49, no.1, pp. 164-179, Jan. 2003.

[7] N. Al-Dhadhir, “Single-carrier frequency domain equalization for space time block coded transmission over frequency selective fading channels,” *IEEE Communication Letters*, vol. 5, pp. 304-306, July 2001.

[8] N. Al-Dhadhir, “Overview and comparison of equalization schemes for space-time-coded signals with application to EDGE,” *IEEE Trans. Signal Processing*, vol. 50, no.10. pp. 2477-2488, Oct. 2002.

[9] H. Mheidat, M. Uysal and N. Al-Dhahir, “Time- and frequency-domain equalization for Quasi-orthogonal STBC over frequency-selective channel,” *IEEE International conference on communications*, Vol.2, pp. 697-701, June 2004.

[10] G. White, J. Correia, Y. Zakharov and A. Burr, “Time-reversal space-time block coded WCDMA receiver in urban and suburban environments,” *IEE Proc-Commun.*, Vol. 152, No.6, pp.1047, 1054, Dec. 2005

[11] P. Xiao, R. Carrasco and I. Wassell, “Time reversal space-time block coding for FWA systems”, *International conference on wireless and mobile communication*, pp.51-55, July 2006.

[12] H. Mheidat, M. Uysal and N. Al-Dhahir, “Quasi-orthogonal time-reversal space-time block coding for frequency-selective fading channels,” *IEEE Trans. On Signal Processing*, vol. 55, no. 2, pp. 772-778, Feb. 2007.

[13] Y. Zhu and K. B. Letaief, “Single-carrier frequency-domain equalization with decision-feedback processing for time-reversal Space-time block coded systems”, *IEEE Trans. on Communications*, vol. 53, no. 7, pp.1127-1131, July 2005.

[14] T. W. Yune, C.H. Choi, and G. H. Im, “Single carrier frequency-domain equalization with transmit diversity over mobile multipath channels,” *IEICE Trans. Commun.*, vol. E89-B, pp. 2050-2060, July 2006.

[15] W. M. Younis et al, “Efficient adaptive receivers for joint equalization and interference cancellation in multi-user space-time block-coded systems,” *IEEE Trans. on Signal Processing*, vol. 51, no.11. pp. 2849-2861, Nov. 2003.

[16] W. M. Younis, "Efficient receivers for space time block coded transmission over broadband channels," PhD Thesis, UCLA, USA, 2004.
[17] W. C. Jakes ,"Microwave mobile communications," NY, Wiley, 1974.
[18] S. Haykin, "Adaptive filter theory," Prentice Hall, 1986.
[19] T. K. Moon, and W. C. Stirling, "Mathematical methods and algorithms" Prentice Hall, 2000.
[20] H. H. Zheng and L. Tong "Blind channel estimation using second order statistics: algorithms," *IEEE Trans. on Signal Processing*, vol.45, no.8. pp.1919-1930, 1997.
[21] I. D. Marsland , "Iterative noncoherent detection of differentially encoded M-PSK," PhD Thesis, University of British Colombia, Canada, 1999.